NRIAG Journal of Astronomy and Geophysics (2016) 5, 173–185

National Research Institute of Astronomy and Geophysics

NRIAG Journal of Astronomy and Geophysics

www.elsevier.com/locate/nrjag

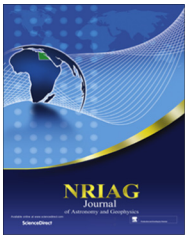

The contribution of gravity method in geothermal exploration of southern part of the Gulf of Suez–Sinai region, Egypt

H. Atef [a,*], A.M.S. Abd El-Gawad [a], M. Abdel Zaher [b], K.S.I. Farag [a]

[a] *Geophysics Department, Faculty of Science, Ain Shams University, 11566 Cairo, Egypt*
[b] *National Research Institute of Astronomy and Geophysics (NRIAG), 11421 Helwan, Cairo, Egypt*

Received 15 April 2015; revised 21 February 2016; accepted 21 February 2016
Available online 29 March 2016

KEYWORDS

Heat flow;
Bouguer map;
Gulf of Suez;
Bottom hole temperature logs;
Gravity inversion

Abstract The Gulf of Suez region represents the most promising area in Egypt for geothermal exploration which is characterized by superficial thermal manifestations represented by a cluster of hot springs with varying temperatures from 35 to 72 °C. The main purpose of the present study was to shed the light on the integration between gravity work and geothermal data in detecting the main subsurface structures in addition to expecting the geothermal sources in the area under consideration.

Correction was applied on the bottom hole temperature data to obtain the true formation equilibrium temperatures that can provide useful information about the subsurface thermal regime. Based on these logging data, temperature gradient and heat flow values were computed at each well, and it is found that the mean geothermal gradient of the study area is 32 °C/km; nevertheless, some local geothermal potential fields were located with more than 40 °C/km. Also, heat flow values are ranging from 45 to 115 mW/m^2.

The Bouguer anomaly map of the study area was used for delineating the subsurface structures and tectonic trends that have resulted in a potential heat source. The gravity inversion revealed a good correlation between areas of high temperature gradients, high heat flow and positive gravity anomalies. The high temperature gradient and heat flow values suggested being associated with a noticeable hydrothermal source of heat anomaly located at relatively shallow depths which is expected to be due to the uplift of the basement in the area.

* Corresponding author.

Peer review under responsibility of National Research Institute of Astronomy and Geophysics.

ELSEVIER Production and hosting by Elsevier

1. Introduction

The Gulf of Suez and the Red Sea together with the Gulf of Aqaba are structurally and genetically closely related. They form the northern branches of the great East African Rift System (Fig. 1). Nearly most of the hottest springs in Egypt

http://dx.doi.org/10.1016/j.nrjag.2016.02.005

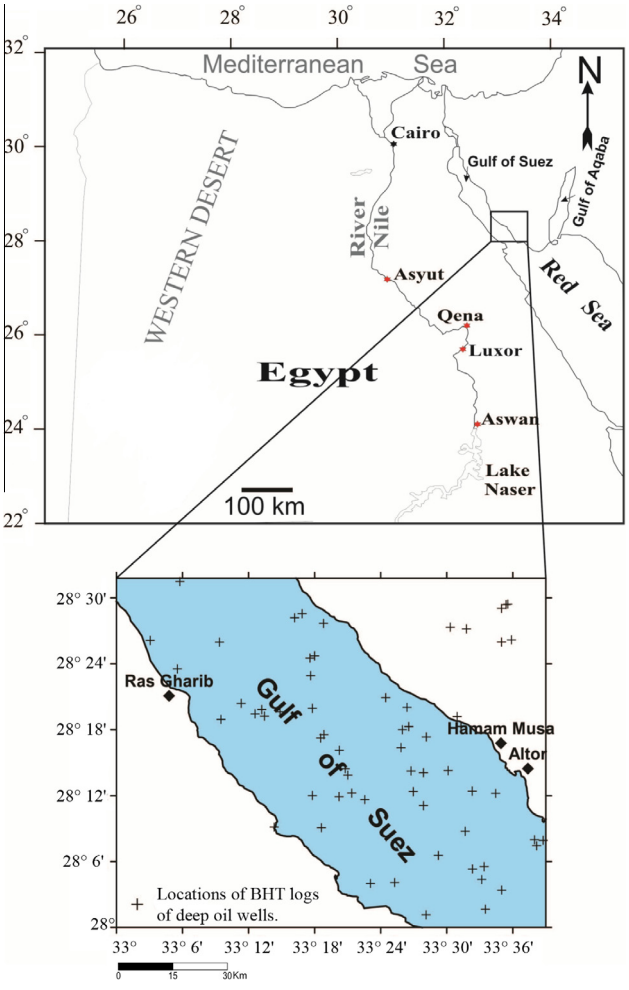

Figure 1 The location map of the study area.

are detected around the coastal parts of the Gulf of Suez, and these springs owe their existence to tectonics (or volcanic) heating associated with the opening of the Red Sea/Gulf of Suez rift (Boulos, 1990).

Since, the thermal activity around Gulf of Suez is controlled by the structural elements affecting the whole gulf area, geophysical approach in the form of gravity method is applied to clarify and manifest the shallower and deeper structural-tectonic setting at the southern part of the Gulf of Suez–Sinai region, Egypt. Moreover, geothermal approach in the form of bottom-hole temperature logs (BHT) is used in an attempt to assist the geothermal potential of the southern part of the study area based on the bottom hole temperature logs of 72 onshore and offshore deep oil wells.

Many geothermal explorations were conducted in Egypt using thermal gradient-heat flow and groundwater temperature-chemistry techniques as well as geophysical tools. Morgan and Swanberg (1979) showed high heat flow values, up to 175 mW/m^2, approximately three times the normal values, in the eastern Egypt, and the heat flow appears to increase toward the Red Sea coast. Also, Morgan et al. (1983) discovered a regional thermal high and a local thermal anomaly along the eastern margin of Egypt. Moreover, Abdel Zaher et al. (2011) evaluated potential geothermal resources in the Gulf of Suez region using both bottom-hole temperature data and geophysical data. Furthermore, Abdel Zaher et al. (2012a) developed conceptual and numerical models of the geothermal system at Hammam Faraun area and demonstrated that Hammam Faraun hot spring originates from a high heat flow and deep groundwater circulation in the subsurface reservoir that are controlled by faults.

Abdel Zaher et al. (2012b) listed stable isotopes of ^{18}O and Deuterium of thermal water samples that were collected from hot springs of Ayun Musa, Hammam Faraun and Hammam Musa. Abdel Zaher suggested that recharge to the hot springs may not be entirely from the Gulf of Suez water, but possibly

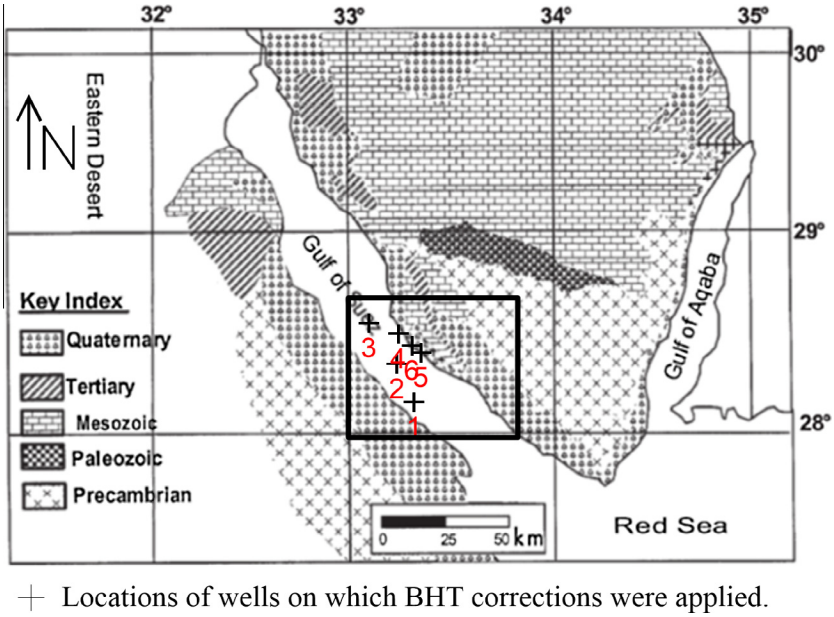

Figure 2 Geological map of the study area after EGSMA (1993).

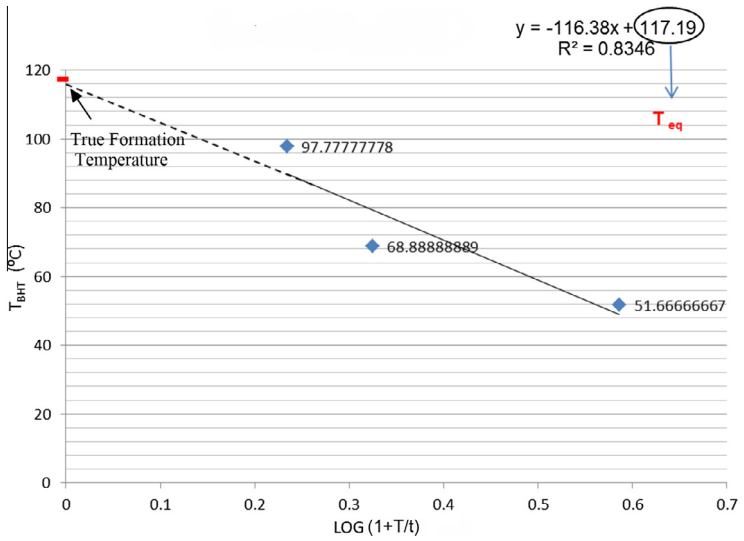

Figure 3 Example of the correction of BHT using the Horner method.

Table 1 Results of some BHT after correction using Horner method (1951) and Waples et al. method (2004).

Well no.	Depth (m)	BHT (Measured) (°C)	$T_{corrected}$ (Horner) (°C)	$T_{corrected}$ (Waples) (°C)
1	2988.56	97.77	118.33	117.2
2	3032.76	100.55	116.53	120.9
3	3824.63	104.44	130.1	126.5
4	3223.56	103.33	128.6	130.7
5	4124.55	123.88	152.6	145.44
6	3687.16	131.11	150.45	150.5

Table 2 Thermal conductivity measured in the southern part of the Gulf of Suez by Morgan et al. (1983).

Description	Conductivity (W/m/K)	No. of samples
Siltstone	2.1	1
Siltstone/sandstone	2.7	1
Carbonate/shale/sandstone	2.4	1
Evaporite/shale	2.3	1
Evaporite	3.3	1
Granite basement	3.1	2

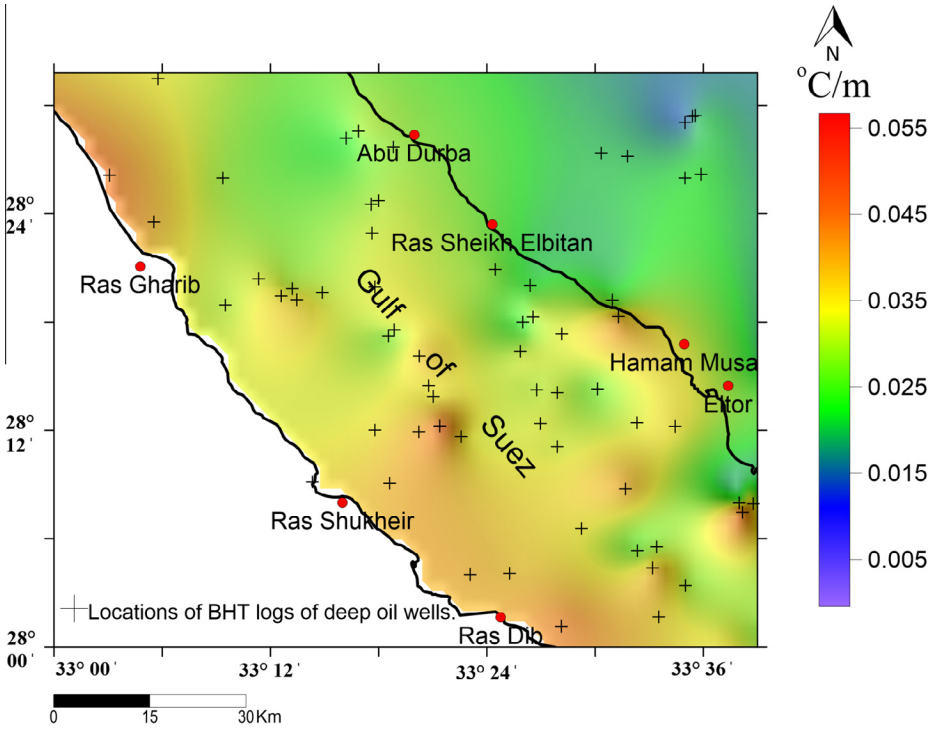

Figure 4 Geothermal gradient map of the study area.

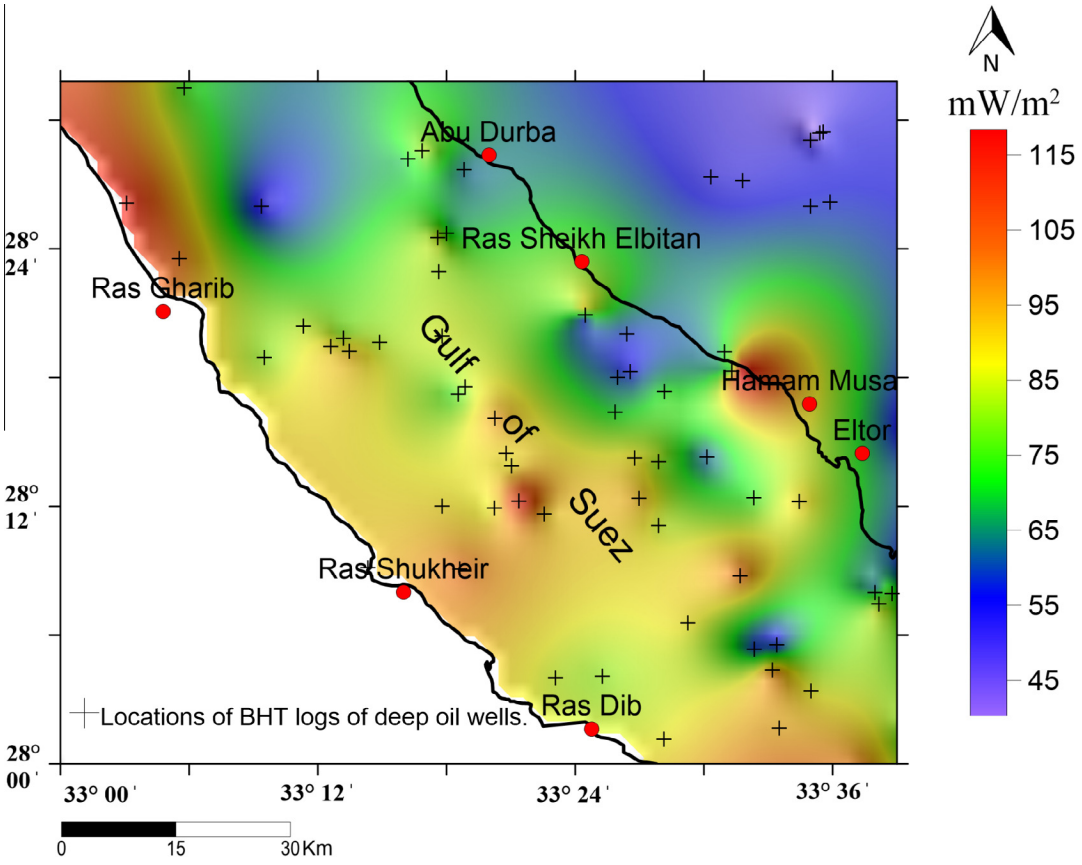

Figure 5 Heat flow map of the study area.

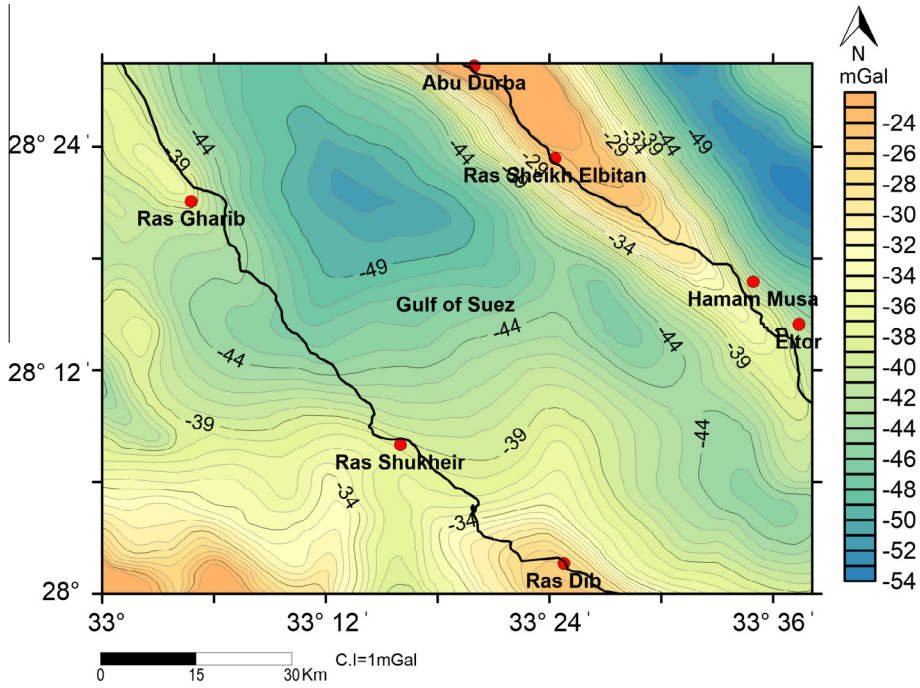

Figure 6 Bouguer map of the study area (GPC, 1976).

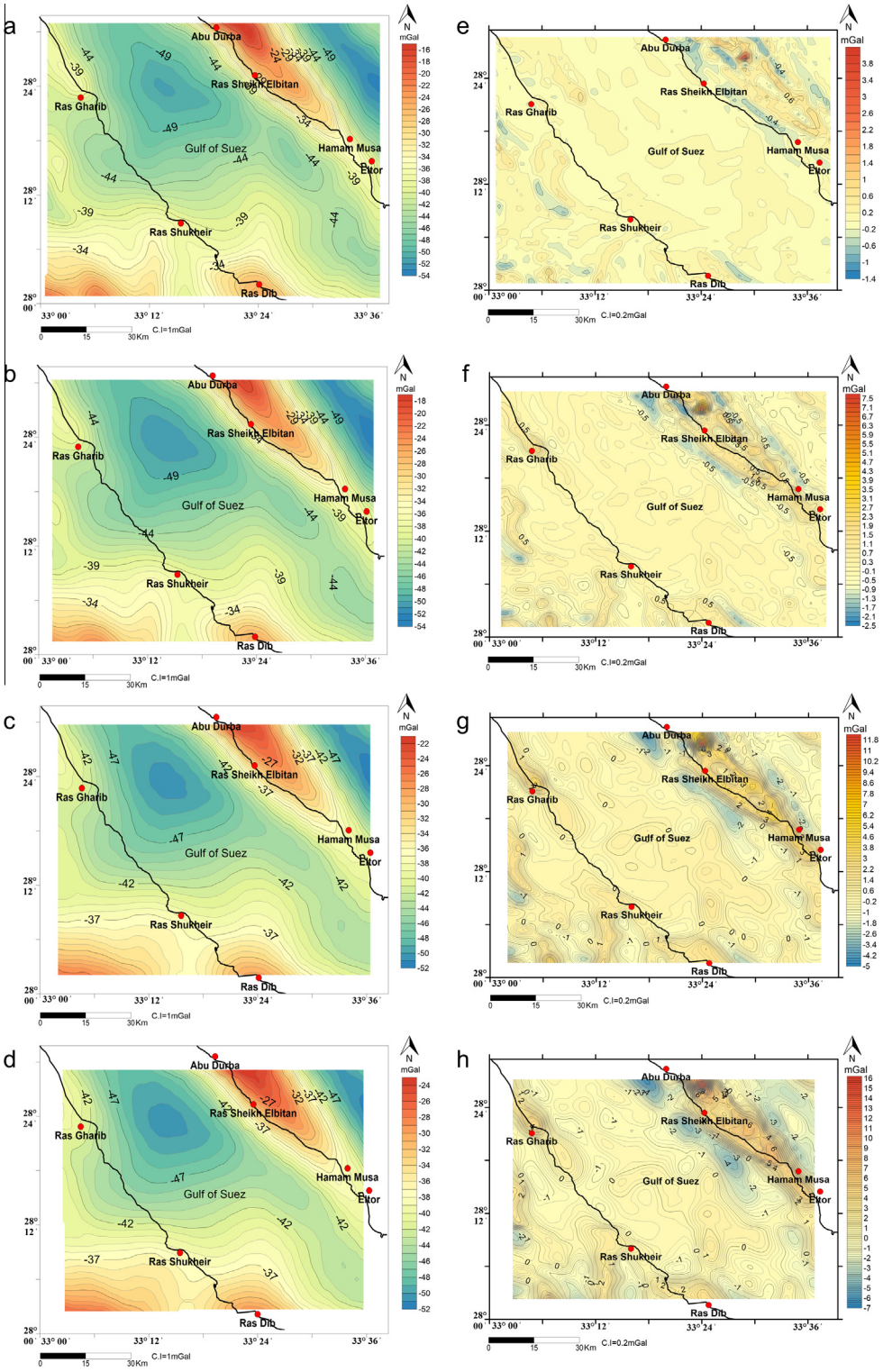

Figure 7 Regional and residual maps at depths from 1 to 4 km using Griffin's method (Griffin, 1949).

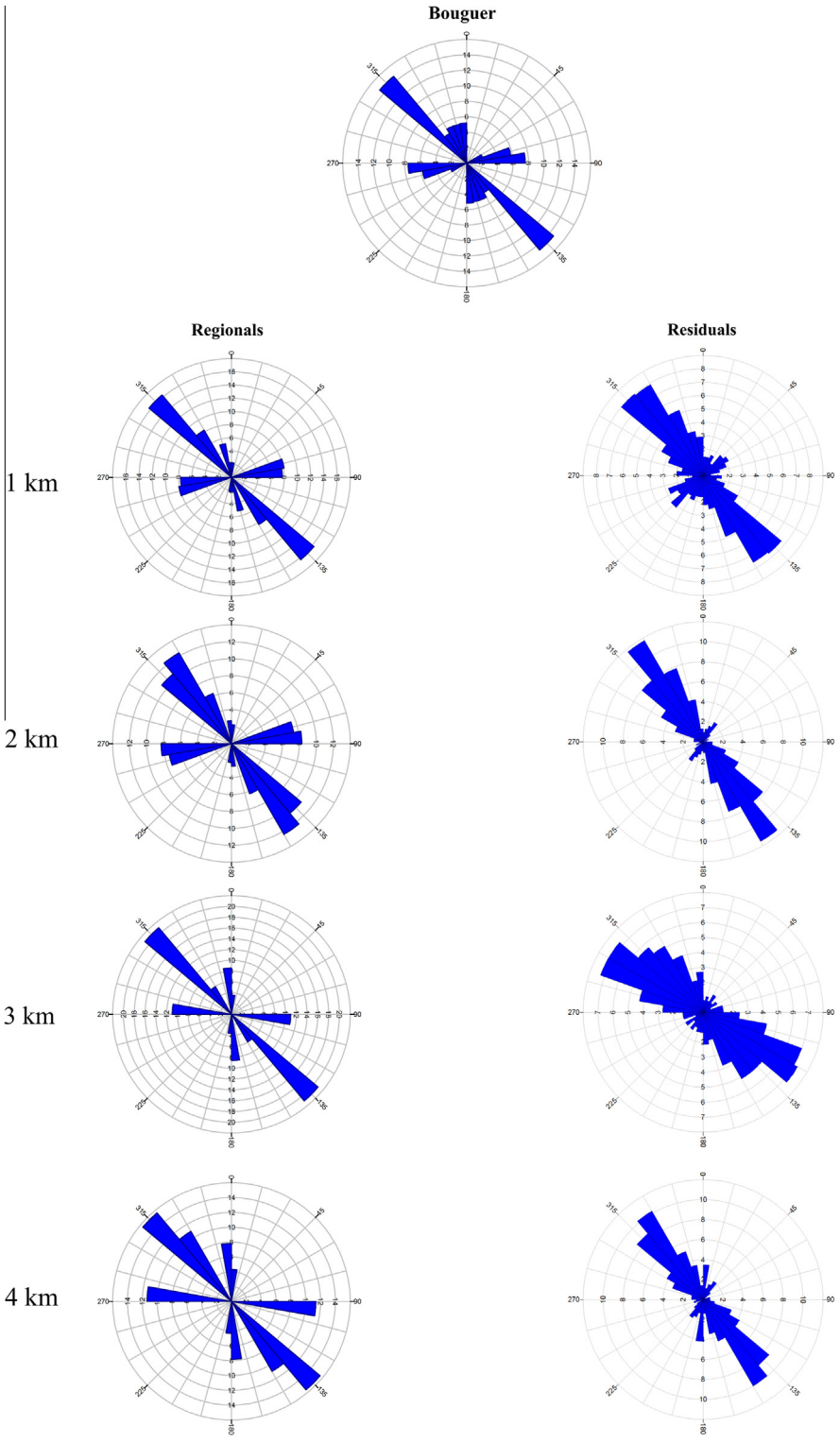

Figure 8 Tectonic trends derived from Bouguer, regional and residual maps of the study area.

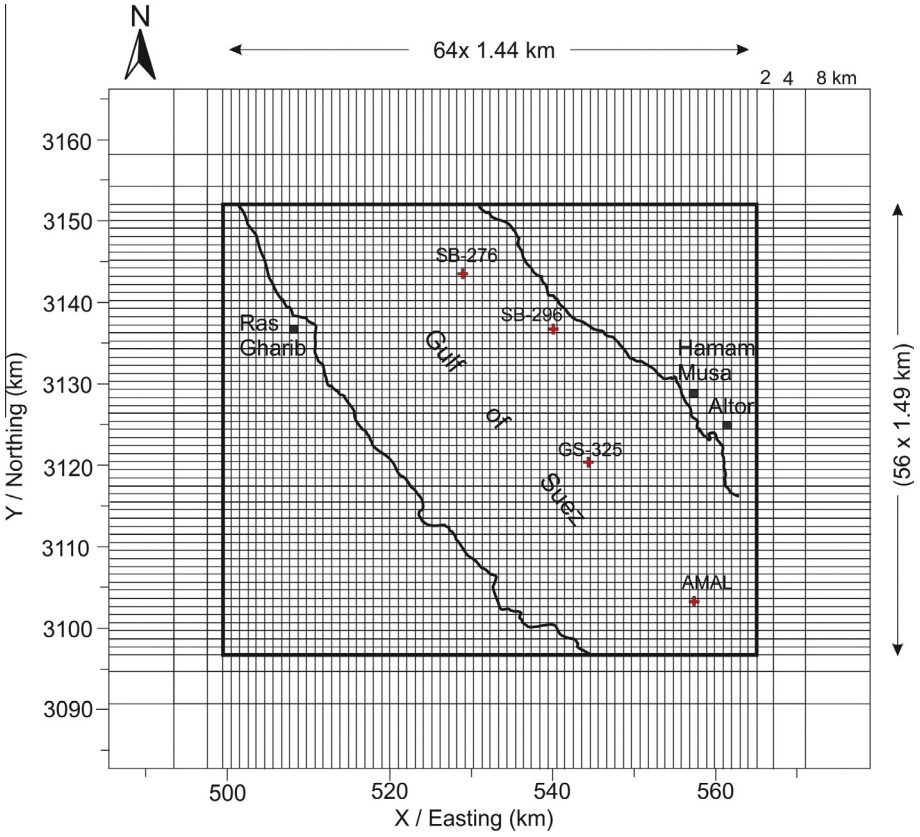

Figure 9 Plain view of the grid blocks for the comprehensive 3D gravity model of the Sothern of Gulf of Suez.

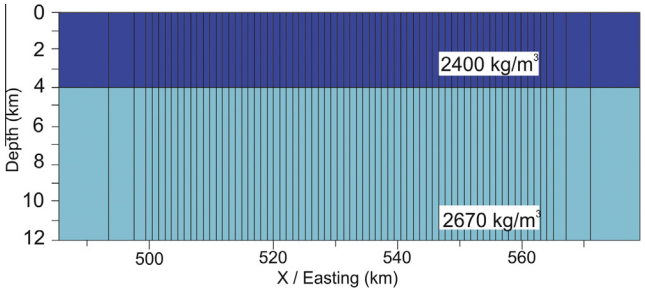

Figure 10 The E–W slice shows the *x*-section of two subsurface layers: sedimentary and basement rocks.

from the meteoric water that comes from areas of higher altitude surrounding the hot springs.

2. Geologic settings

The geology of the area (Fig. 2) ranges from Precambrian basement rocks to the Quaternary deposits. According to the Egyptian Geological Survey map (EGSMA, 1993), the Quaternary deposits cover the basement rocks along the Gulf of Suez and Gulf of Aqaba. The basement rocks (Precambrian) occupy the southern part of the study area, along the Gulf of Suez and Gulf of Aqaba. On the other hand, the Paleozoic rocks are present in the middle part while the Mesozoic rocks covered the eastern and western parts of the area (Rabeh et al., 2003).

The Southern Sinai lies between the eastern and western flanks of the Red Sea Gulf rifts and it has been subjected to intensive faulting during the rift activities. There are two main fault structures, the first one runs along the contact between the sedimentary section and the basement complex, while the second one runs along the Gulf of Suez coast to the west (Abdallah and Abu Khadra, 1976).

3. Geothermal studies

Geothermal approach in the form of bottom-hole temperatures (BHT) is used in an attempt to assist the geothermal potential of the southern part of Gulf of Suez–Sinai region based mainly on temperature data from 72 deep onshore oil wells, with depths ranging from 1200 to 4700 m. These measurements were carried out by oil companies, including the Egyptian General Petroleum Company (EGPC), the Gulf of Suez Petroleum Company (GUPCO), and British Petroleum Company (BPC).

The temperature data are in the form of bottom-hole temperature (BHT) which is measured at the bottom of the well. Temperature logs are routinely measured during drilling or soon after circulation has ceased. Thus, these data are typically lower than the true temperature of the formation due to the cooling effect of drill fluid circulation. The cold drilling fluid invades the formation and cools it down very efficiently via

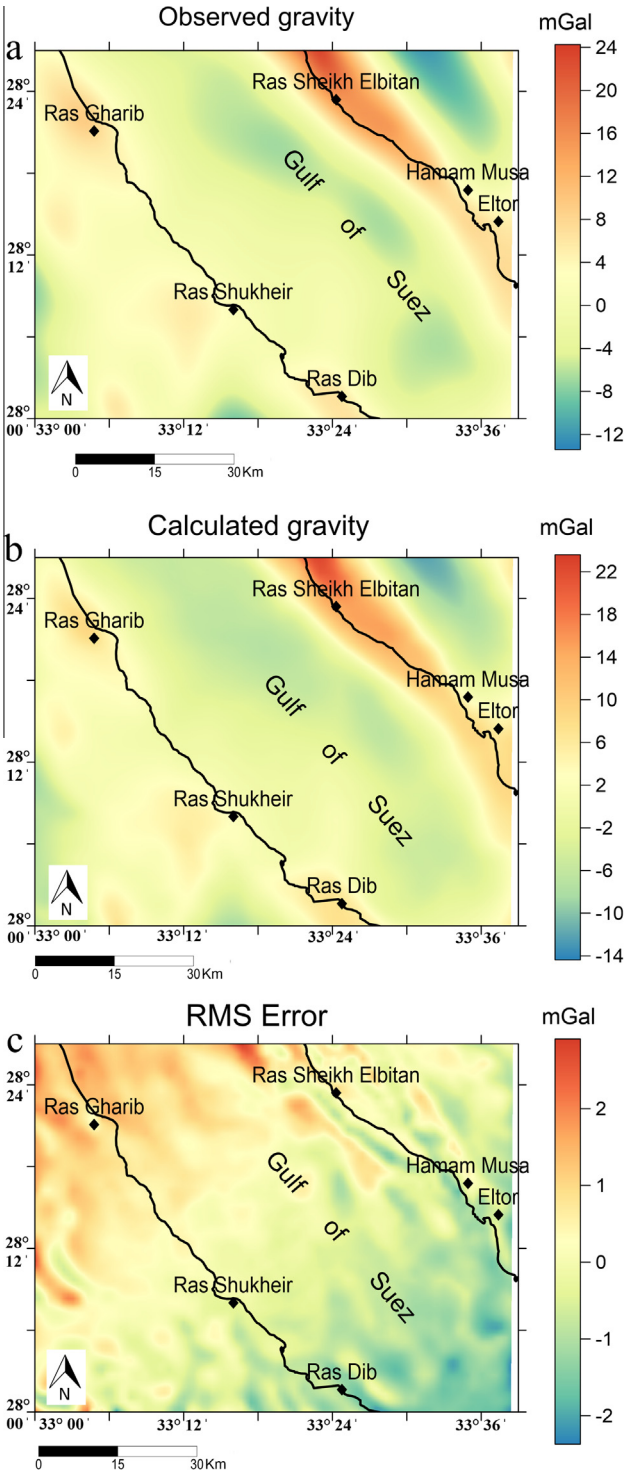

Figure 11 Resulted 3D gravity inversion maps of the study area.

heat convection. It is defined by the cooling effect of the drilling fluid and the heating effect of the formation. When the circulation of the drilling mud stops, the borehole gradually regains the true formation temperature.

Several methods have been used to correct the logged BHT to real formation temperatures. BHT were corrected by using two methods Waples et al. (2004) and Horner methods (1951), to obtain the true Formation Temperature (FT), which is an essential parameter to determine the temperature gradient and heat flow. Horner method (1951) is recommended if three of more self-consistent BHT from a given depth are available.

It assumes that the wellbore can be considered as a linear source of heat so that the thermal effect of drilling is approximated by a constant linear heat source. Horner correction was applied using the following formula:

$$T_{eq} = T_{BHT} + A \cdot \log(1 + T/t) \quad (1)$$

where T_{eq} is the corrected temperature at equilibrium (°C), T is the time of cooling which is assumed to be 10 h as the mud circulation less than this time has a negligible effect, "t" is the time since circulation which is in hours and T_{BHT} is the measured bottom hole temperature in Celsius (°C) (Fig. 3).

Waples et al. (2004) method is used for correcting log-derived temperatures in deep wells (3500–6500 m) by comparing log temperatures from the Gulf of Campeche (Mexican Gulf of Mexico) with Drill Stem Test (DST) temperatures in the same wells. The equations developed are modified slightly from those of Waples and Mahadir (2001), which were calibrated using data from depths less than 3500 m in Malaysia. The correction depends strongly on time since end of mud circulation (TSC) and, to a much lesser degree, on depth. The corrected subsurface temperature (Celsius) is given by

$$T_{true} = T_{surface} + f_s \cdot (T_{measured} - T_{surface}) - 0.001391(Z - 4498) \quad (2)$$

where $T_{measured}$ is the measured log temperature in Celsius, Z is depth below seafloor in meters and $T_{surface}$ is the seafloor or land surface temperature which is taken as 26.7 °C. The correction factor, f, is a function of TSC which equals

$$f_s = (-0.1462 * \ln(T_{sc}) + 1.699)/(0.572 * Z^{0.075}) \quad (3)$$

According to the two aforementioned methods, we found the results are approximately similar as shown in Table 1.

After correcting the bottom hole temperature data, the geothermal gradient of each well is calculated and plotted together to determine the mean temperature gradient of the study area taking the main surface temperature to be 26.7 °C using the following equation:

$$G.G = \Delta T/\Delta Z = T_2 - T_1/Z_2 - Z_1 \quad (4)$$

where G.G. is the geothermal gradient (°C/m) and ΔT is the temperature change in a depth interval of $Z_2 - Z_1$ (m).

Accordingly, the mean geothermal gradient of the area is 0.032 (°C/m) while the maximum gradient is found to be 0.045 °C/m around Hamam Musa and Ras Gharib areas as shown in Fig. 4. Also, heat-flow values are determined using the equation below by combining sets of temperature gradient and thermal conductivity data calculated by Morgan et al. (1983) (Table 2)

$$Q = K(dt/dz) \quad (5)$$

where 'Q' is heat flow in mW/m^2, 'K' is thermal conductivity in W/m °C, and 't' is temperature in Celsius at depth z in meters.

Thus, the regional heat flow of the study area is ranging from 45 to 115 mW/m^2 while the maximum value encountered near Hamam Musa and Ras Gharib areas is 117.13 mW/m^2 (Fig. 5). High values of both geothermal gradient and heat flow of such areas suggest a noticeable heat anomaly located

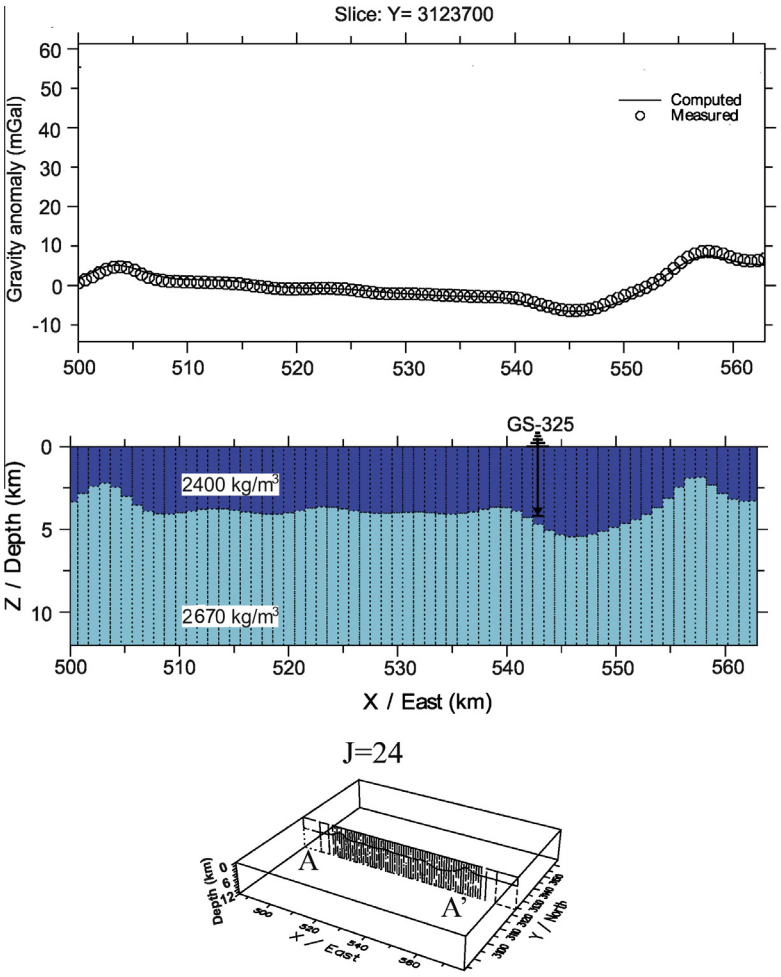

Figure 12 2D gravity inversion section across profile A–A′.

at relatively shallow depths, probably due to the uplift of the basement in the area.

4. Gravity interpretation

Gravity data in the form of Bouguer anomaly map are used to infer the geologic characteristics and delineate the subsurface structures of the study area. The Bouguer anomaly map of the study area, a scale of 1:100,000 with 1 mGal contour interval, is compiled by the General Petroleum Company (1976). Such a Bouguer anomaly map (Fig. 6) is characterized by the presence of four gravity belts of varying polarities: most northern incomplete gravity low belt, north eastern gravity high belt, large central gravity low belt and southern incomplete gravity high belt.

To enhance the structural features from the sedimentary and basement rocks in the study area, gravity data were isolated into regional and residual components. The separation process was performed using Griffin method (1949) to identify the residual features from those of regional nature at different depths from 1.0 km to 4.0 km.

The regional gravity anomaly map (Fig. 7a) is mostly identical in the anomalies polarities, trends, shapes and areal extension and reveals simpler and smoother contours than the Bouguer anomaly map. The interpretation of regional gravity maps from 1.0 km to 4.0 km (Fig. 7a–d) shows that, the local anomalies are merging together to form larger ones, and the contour gradients decrease due to the decrease of density contrast between sedimentary section and basement complex. In addition to that the anomalies became broader and wider.

The interpretation of residual gravity maps from 1.0 km to 4.0 km (Fig. 7e–h) shows that, the relief increases gradually with depth, the local anomalies are merging together to form larger ones, and the contour gradients increase due to the increase of density contrast between sedimentary section and basement complex. In addition to that the anomalies became broader and wider.

5. Tectonic trend analysis

The main tectonic trend derived from Bouguer, regional and residual gravity maps (Fig. 8) revealed that the main tectonic trend is the NW–SE trend (Red Sea system) during the Early Tertiary (Abdel Gawad and Ibraheem, 2005). Thus, the tectonic trend for shallower and deeper sections is the same which gives an indication to vertical uplift movement rather than the

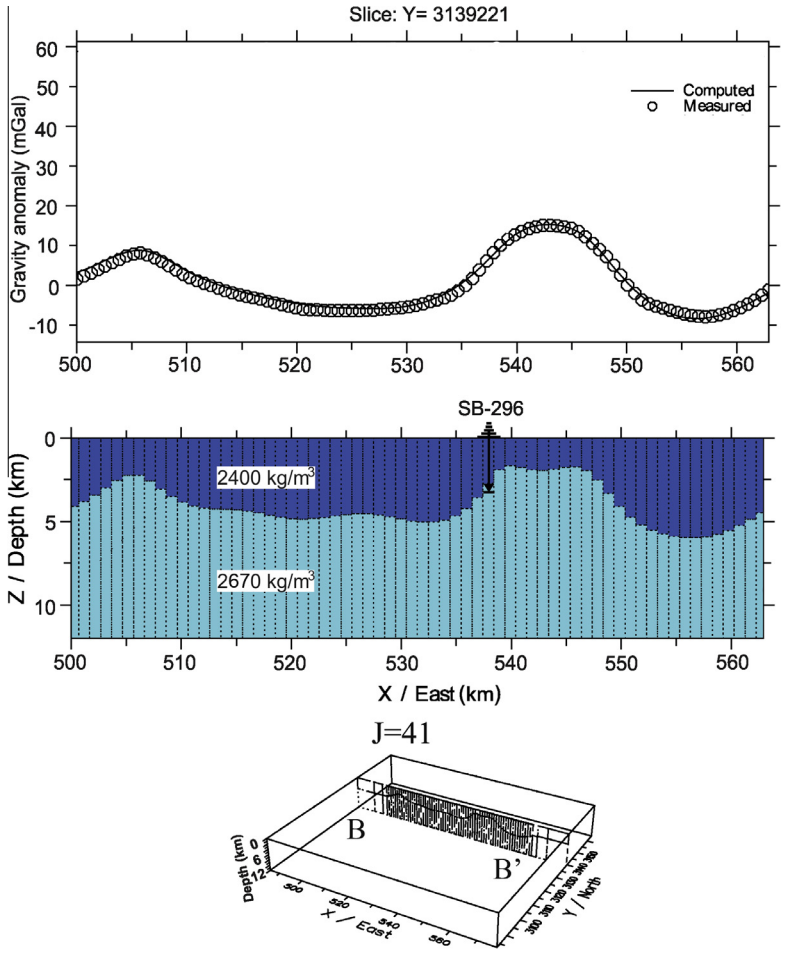

Figure 13 2D gravity inversion section across profile B–B′.

lateral compression. This is clear from the predominant NW–SE trend of the Red Sea/Gulf-of-Suez.

6. Gravity inversion

The aim of gravity inversion is to determine the density distribution that would explain the measurements and/or the shape and dimensions of density variations. The gravity effect of this 3D crustal model for the study area has been computed using GRABLOX-1.7 and BLOXER-1.5 softwares developed by Markku Pirttijärvi, University of Oulu, Finland (Pirttijärvi, 2004). GRABLOX program computes the synthetic gravity anomaly of a 3D block model while BLOXER program was used for model editing and visualization.

The model of study area covers 3800 km^2 and was oriented in a north–south direction, extending 64 km in the east–west direction and 56 km in a north–south direction. The special discretization was 68 grid blocks in the east–west direction (‘*i*’ index) and 59 blocks in the north–south direction (‘*j*’ index). The area is divided into several blocks each of dimension 1.44 km and 1.49 km in the E–W and N–S directions (Fig. 9).

The model is based on two-layer case; sedimentary cover has an average density of 2.4 g/cm^3 and basement complex has an average density of 2.67 g/cm^3 (Fig. 10). Margins are important in gravity data interpretation using two layer model with constant density contrast. The margins extend the edge effect of the top most layers away from the computation area which is called the Buffering effect. Thus, the new margins extend to 8 km more than the Bouguer area to accurately model the study area. Also, the regional field is optimized in order to find out the gravity effect of only masses that are located inside the volume of model without the effect of masses that are located around and below the study volume.

The results of the 3D gravity inversion are shown in Fig. 11. The comparison of the original Bouguer anomaly map with that calculated for the crustal model shows considerable similarities. When comparing the observed gravity and the modeled gravity of the study area, it is found that the Root Mean Square (RMS) Value of the performed model is 0.022. The optimized models of some sections for both the observed and calculated gravity anomalies as well as the computed regional field are plotted.

The resulted sections show considerable confirmation between the true depths from some oil wells (GS-352, SB-296 and SB-276) with the depths computed from 3D block model of gravity data (Figs. 12–14). Also, it is very important to mention that the east–west section along Hammam Musa hot

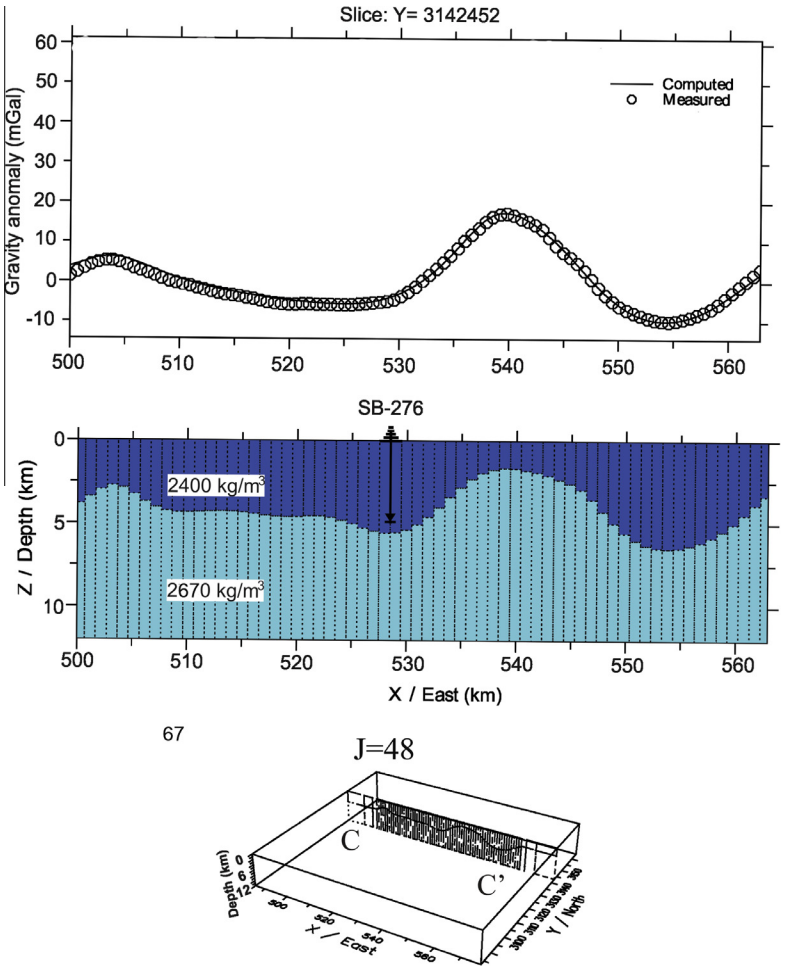

Figure 14 2D gravity inversion section across profile C–C′.

spring suggested that the origin of this spring is due to vertical uplift of the basement rock (Fig. 15).

The 3D basement depth map of the area under investigation (Fig 16) shows that the depth to basement ranges between 1000 and 4600 m. However, it is important to mention that the depth to the basement in the northeastern part of the study area is relatively shallower (1200 m), which reveals a considerable vertical uplift at this location. This uplift of basement correlates with areas of high temperature gradient and heat flow.

7. Results and discussion

Integration between both gravity and geothermal studies has been emphasized in which the areas of high geothermal gradients and heat flow values correlate well with high positive gravity anomalies. 3D modeling of the gravity data seems to work efficiently and is capable of detecting the interface between the basement rock and the sedimentary cover. The correlation between 3D basement surface derived from gravity modeling and the geothermal gradient map (Fig. 17) suggests that the uplifted basement blocks are the source of heat in the study area. Therefore, the thermal maturity lines the study part of the Gulf of Suez would reflect basement structure. Accordingly, the uplifted basement rock is the site of high temperature gradient and heat flow. Thus, tectonic uplift of hotter rocks (basement) causes deep fluid circulation of groundwater through the faults and fractures on the surface of the basement rock and causes increase of temperature gradient and heat flow values.

8. Summary and conclusions

Geothermal studies based on bottom-hole temperature logs of 72 onshore oil wells show that the mean geothermal gradient of the study area is 32 °C/km which reflects low geothermal potentiality. However, some local geothermal potential fields were encountered with moderately high temperature gradient (> 40 °C/km) and high heat flow is ranging from 115 mW/m^2. Also, geophysical studies based on gravity data in the study area were analyzed to delineate the shallower and deeper structural-tectonic setting in the southern part of the Gulf of Suez and to constrain origin of the heat sources at the hottest areas.

Gravity lineaments suggested that the major deeper regional trend is NW–SE trend (Red Sea system) during the Early Tertiary which is derived from Bouguer and regional gravity maps which is the same as major shallower local trend that is derived from residual gravity maps.

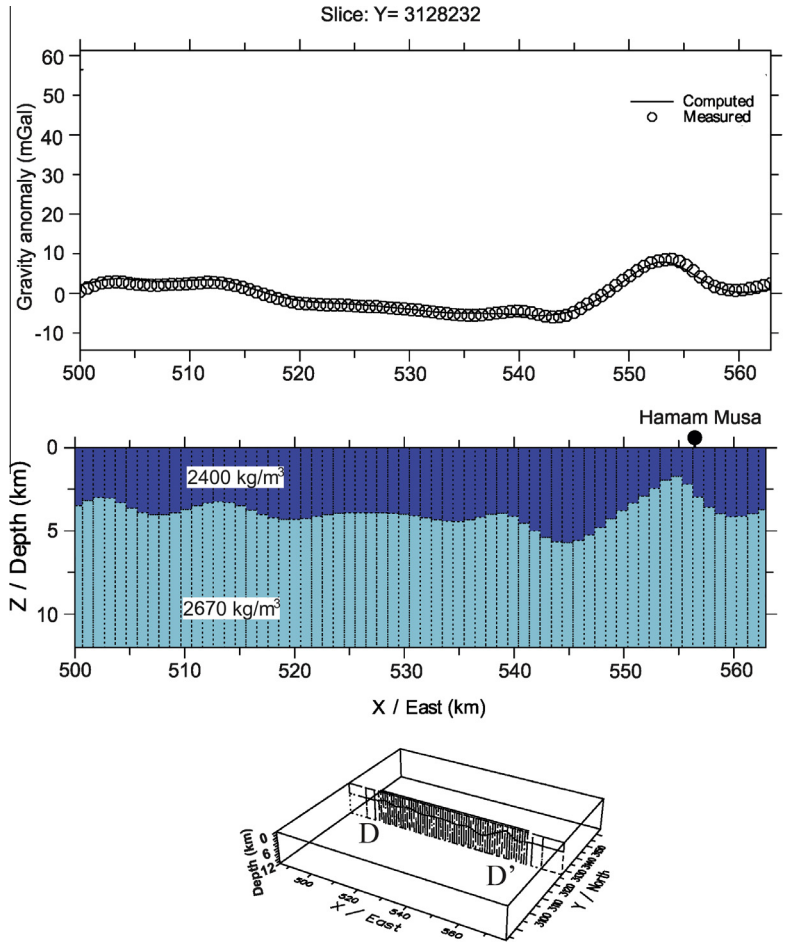

Figure 15 2D gravity inversion section across profile D–D′.

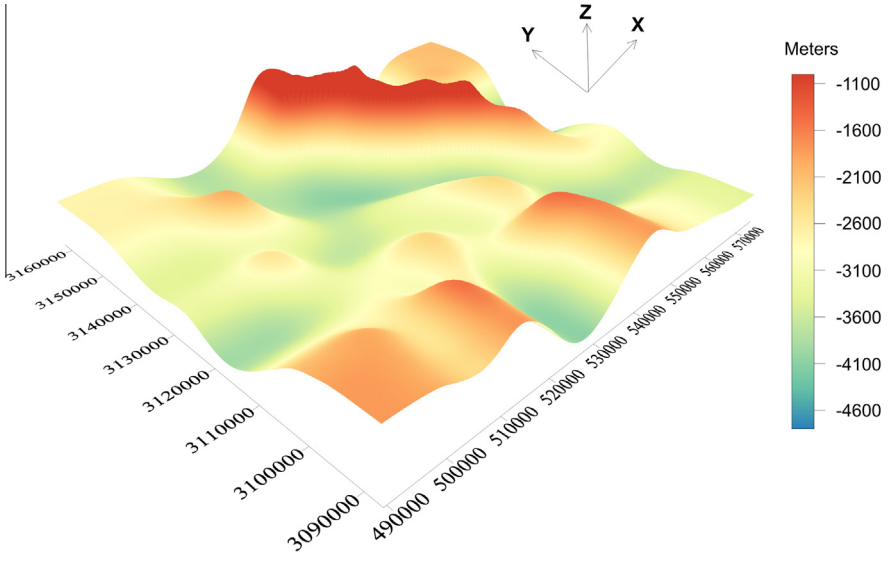

Figure 16 3D basement depth view of the study area resulted from gravity inversion.

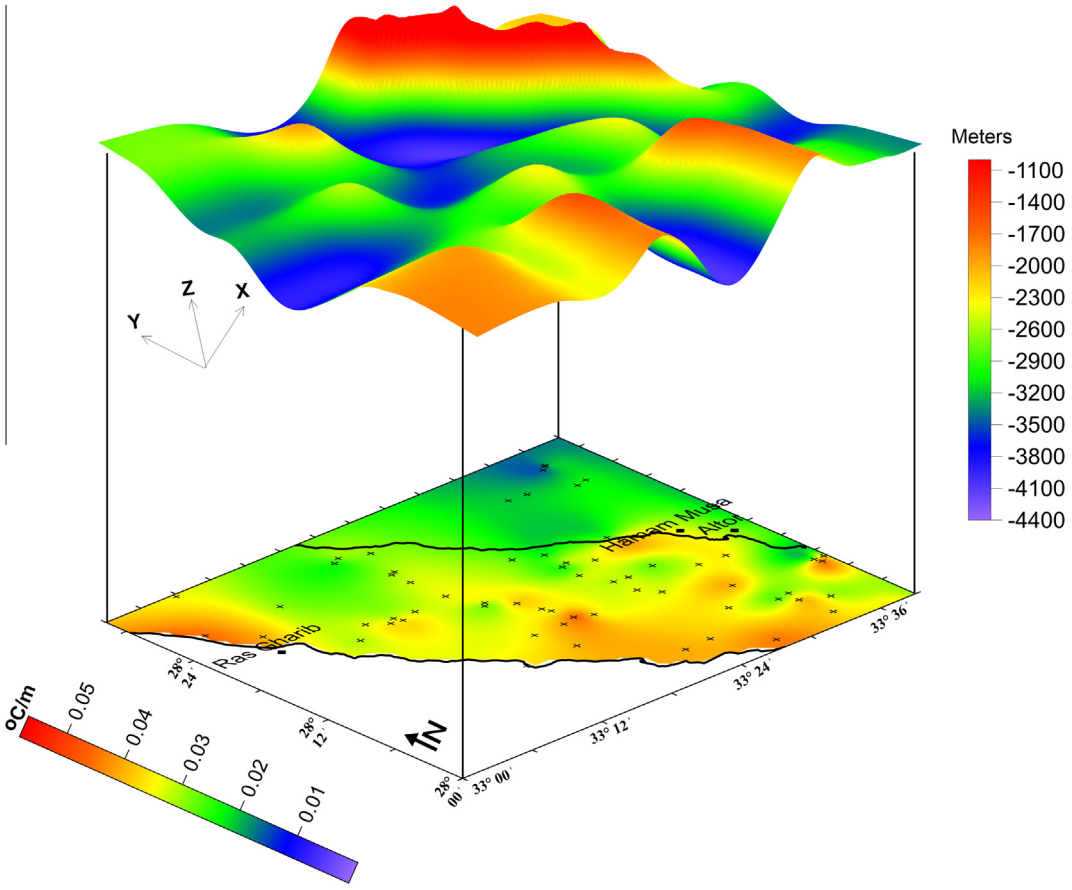

Figure 17 Integration between the resulted depth to basement and geothermal gradient maps of the study area.

Integration of geophysical data and geothermal data shows a good correlation between areas of high heat flow and positive gravity anomalies which implies that the geothermal potential in the southern part of Gulf-of-Suez is controlled by uplifts and faults on the basement rocks. Thus, this result can be used also for eliciting the source of hot springs that is due to tectonic uplift of hotter basement rocks causing deep fluid circulation through faults on the surface of the basement rock. Such faults allow the formation of discharging conduits for water ascending from depth after being heated and mixed with other water type. In other words, the uplifted basement is the site of high heat flow.

References

Abdallah, A.M., Abu Khadra, A.M., 1976. Remark on the geomorphology of the Sinai Peninsula and its associated rock, Egypt. Geol. Surv., Egypt.

Abdel Zaher, M., Saibi, H., El Nouby, M., Ghamry, E., Ehara, S., 2011. A preliminary regional geothermal assessment of the Gulf of Suez, Egypt. J. Afr. Earth Sci. 60, 117–132.

Abdel Zaher, M., Saibi, H., Nishijima, J., Mesbah, H., Fujimitsu, Y., Ehara, S., 2012a. Exploration and assessment of the geothermal resources in the Hammam Faraun hot spring, Sinai Peninsula, Egypt. J. Asian Earth Sci. 45, 256–267.

Abdel Zaher, M., Saibi, H., Ehara, S., 2012b. Geochemical and stable isotopic studies of Gulf of Suez's hot springs, Egypt. Chin. J. Geochem. 1, 120–127.

Abdel Gawad, A.M., Ibraheem, I.M., 2005. Gravity-deduced faults associated with the Northern Sinai Syrian arc folds M.E.R.C. Ain Shams Univ., Earth Sci. Ser. 19, 165–178.

Boulos, F., 1990. Some aspects of the geophysical regime of Egypt in relation to heat flow, groundwater and micro earthquakes. In: Said, R. (Ed.), The Geology of Egypt. Balkema, Rotterdam, pp. 407–438

EGSMA (Egyptian Geological Survey and Mining Authority), 1993. Geologic Map Sinai, Egypt (scale 1:100 000).

GPC (General Petroleum Company), 1976. Bouguer Map of El Tor Area, Sinai, Egypt (scale 1:100 000).

Griffin, W.R., 1949. Residual gravity in theory and practice. Geophysics 14, 39–56.

Horner, R.D., 1951. Pressure build-up in wells. Proc. Third World Petroleum Congress, The Hague, 34: 316.

Morgan, P., Swanberg, C.A., 1979. Heat flow and the geothermal potential of Egypt. Pageoph 117, 213–226.

Morgan, P., Boulos, K., Swanberg, C.A., 1983. Regional geothermal exploration in Egypt. EAEG 31, 361–376.

Pirttijärvi, M., 2004. BLOXER. Interactive Visualization and Editing Software for 3-D Block Models, Version 1.5, User's Guide, Geophysical Survey of Finland, Report Q16.2/2004/1.

Rabeh et al., 2003. Structural Set-up of Southern Sinai and Gulf of Suez Areas Indicated by Geophysical Data, 46, No 6.

Waples, D.W., Mahadir, R., 2001. A statistical method for correcting log-derived temperatures. Petrol. Geosci. 7, 231–240.

Waples, D.W., Pacheco, J., Vera, A., 2004. A method for correcting log-derived temperatures in deep wells, calibrated in the Gulf of Mexico. Petrol. Geosci. 10, 239–245.